



# Investigation of the diurnal pattern of the vertical distribution of pollen in the lower troposphere using LIDAR

Y. M. Noh<sup>1</sup>, H. Lee<sup>2</sup>, D. Mueller<sup>1,\*</sup>, K. Lee<sup>3</sup>, D. Shin<sup>1</sup>, S. Shin<sup>1</sup>, T. J. Choi<sup>4</sup>, Y. J. Choi<sup>5</sup>, and K. R. Kim<sup>5</sup>

<sup>1</sup>Department of Environmental Science & Engineering, Gwangju Institute of Science & Technology, Gwangju, South Korea

<sup>2</sup>Department of Spatial Information Engineering, Pukyong National University, Busan, South Korea

<sup>3</sup>Department of Geoinformatics Engineering, Kyungil University, Gyeongsan-si, Gyeongbuk, South Korea

<sup>4</sup>Korea Polar Research Institute, Incheon, South Korea

<sup>5</sup>Applied Meteorology Research Lab, National Institute of Meteorological Research, Seoul, South Korea

\* now at: the University of Hertfordshire, Hatfield, United Kingdom and also at Science Systems and Applications, Inc., NASA Langley Research Center, Hampton, Virginia, USA

Correspondence to: H. Lee (hanlimlee10@gmail.com)

Received: 6 September 2012 – Published in Atmos. Chem. Phys. Discuss.: 5 December 2012

Revised: 2 July 2013 – Accepted: 2 July 2013 – Published: 7 August 2013

**Abstract.** The diurnal pattern of the vertical distribution of biogenic pollen in the lower troposphere was investigated by LIDAR. Meteorological data were taken at the ground. Pollen concentrations were measured at the surface using a Burkard 7-day-recording volumetric spore sampler. Aerosol extinction coefficients and depolarization ratios at 532 nm were obtained from LIDAR measurements in spring (4 May–2 June) 2009 in Gwangju, South Korea. Linear volume depolarization ratios varied between 0.08 and 0.14 and were observed only during daytime (09:00–17:00 local time (LT)) during days of high pollen concentration (4 to 9 May). Daily average pollen concentrations ranged 1000–2500 cm<sup>-3</sup> in the same period. The temporal evolution of the vertical distribution of the linear volume depolarization ratio showed a specific diurnal pattern. Linear volume depolarization ratios of more than 0.06, were measured near the surface in the morning. High depolarization ratios were detected up to 2 km aboveground between 12:00 and 14:00 LT, whereas high depolarization ratios were observed only close to the surface after 17:00 LT. Low values of depolarization ratios ( $\leq 0.05$ ) were detected after 18:00 LT until the next morning. During the measurement period, the daily variations of the high depolarization ratios close to the surface showed correlation to number concentration measurements of pollen. This finding suggests that high depolarization ratios could be attributed to enhanced pollen concentrations. The diurnal characteristics of the high values of depolarization ratios are thought to be

closely associated with turbulent transport. Diurnal and vertical characteristics of pollen, if measured continuously, could be used to improve the accuracy of pollen-forecasting models via data assimilation studies.

## 1 Introduction

Pollen, which are atmospheric particles of biogenic origin, is a common cause of allergy-related diseases such as asthma, rhinitis, and atopic eczema (Lewis et al., 1983; Esch and Bush, 2003). In the industrialized countries of central and northern Europe, up to 15 % of the population is sensitive to pollen allergens (WHO, 2003). Pollen also has adverse effects on the atmospheric environment by decreasing visibility during main pollination seasons. Kim (2007) reports that the average contribution of pollen to visibility impairment is estimated to be 19–25 % during the periods of main pollination. According to previous studies (Beggs, 2004; D'Amato and Cecchi, 2008; Shea et al., 2008), these negative effects of airborne pollen are becoming increasingly problematic as climate change rapidly progresses. In order to understand and predict temporal and spatial characteristics of pollen, various pollen-concentration forecasting models have been developed (Andersen, 1991; Giner et al., 1999; Laaidi, 2001; Adams-Groom et al., 2002; Gioulekas et al., 2003; Laaidi et al., 2003; Water et al., 2003; Vázquez et al., 2003). These

forecasting models utilize pollen concentration data observed by in situ aerobiological monitors near the surface (Frøsig and Forbundet, 2003; Severova and Polevova, 1996; Porsbjerg et al., 2003; Rantio-Lehtimäki and Matikainen, 2002). However, there is convincing evidence that long-range transported pollen can significantly enhance pollen concentrations at both the surface and at elevated altitudes above the receptor sites. Especially in these cases, temporally and vertically resolved data of pollen (concentration measurements) are expected to improve the forecasting capability of these models.

Raynor et al. (1973) and Hart et al. (1994) report that the vertical distribution of the pollen abundance is highly correlated with meteorological conditions. Their findings are based on vertically resolved measurements using towers. Since the maximum height of their sampling was limited to 108 m, these tower-based studies could not properly take account of the distribution of pollen up to the top of the planetary boundary layer and in the free troposphere. Experimental data from sampling of pollen aboard aircraft indicates the presence of substantial pollen concentrations at greater heights. These results corroborate the hypothesis that recurring meteorological conditions favor vertical exchange and long-range transport of pollen (Mandrioli et al., 1984). Although many types of investigations, including airborne and tower-based measurements, have been performed to understand the dispersion and physical behavior of long- and short-range transport of pollen grains (Raynor et al., 1975; Mandrioli et al., 1984; Hjelmroos, 1991; Sofiev et al., 2006), the data obtained from these studies are limited in their representativeness because of, e.g. the limited number of observed pollen events, the lack of continuous airborne measurements, and the limited height coverage of tower-based measurements (Raynor et al., 1974). Therefore, observations of the diurnal variation of the vertical distribution of the abundance of pollen is needed for investigations of pollen dispersion and pollen transport.

Anthesis and pollen release are influenced by the circadian patterns associated with air temperature, relative humidity, and wind speed (Kasprzyk, 2006). Daily temperature and relative humidity act as significant factors that influence the release of pollen into the ambient air (Bartková-Ščevková, 2003). Pollen transport, dispersal and atmospheric concentration of pollen are mainly affected by meteorological factors (Damialis et al., 2005; Sofiev et al., 2006). However, few studies have investigated the vertical distribution of pollen in conjunction with meteorological conditions. Therefore, in order to understand and predict pollen release, dispersal, and transport, it is necessary to simultaneously measure the vertical distribution of pollen and meteorological variables.

The main goal of this study is to understand the vertical characteristics and diurnal patterns of pollen on the basis of the prevailing meteorological conditions via 24 h LIDAR measurements at an urban site during a one-month period when pollen release was most active. To identify the relation of pollen to the linear particle depolarization ratio

measured by LIDAR, we analyzed the surface pollen and  $PM_{10}$  concentrations and AERONET (Aerosol Robotic Network) sun/sky radiometer data. The surface meteorological data (relative humidity, wind speed, and temperature) and radiosonde data were also employed to investigate the relationship between diurnal patterns of the vertical pollen distribution and these meteorological factors. Section 2 describes the measurements. Section 3 explains the relationship between pollen and depolarization ratio. Section 4 discusses the effects of meteorological conditions on diurnal and vertical patterns of pollen. Section 5 closes with a conclusion.

## 2 Measurements

Polarization LIDAR measurements were carried out on the campus of the Institute of Science and Technology (GIST). We used the the Depolarization LIDAR system (DPL) of the Korea Polar Research Institute (KOPRI) during May 2009, which is the main pollen season in Korea (Park et al., 2008). The DPL was located at 35.13° N, 126.50° E. The elevation of the lidar site is 53 m above mean sea level (m.s.l.). The observation site is 50 km away from the coastline and the measurement site is surrounded by forests, buildings, mountains, and farms.

The DPL is equipped with a high-power (170 mJ), 10 Hz pulse repetition rate, Nd:YAG (532 nm) laser. The emitted laser pulses have a divergence of less than 0.3 mrad after they are expanded five-fold with a beam expander. The signal receiver module is an 8-inch Schmidt-Cassegrain telescope. It has a focal length of 2032 mm. The DPL was used with a fixed field of view (FOV) of 2 mrad during the observation period. This value allows for a full overlap between the telescope FOV and the laser beam to a minimum height of around 300 m a.m.s.l. This FOV value, in accordance with the analog-to-digital convertor, enables us to sample signals to distances up to 6 km from the instrument. The temporal and spatial resolution of the DPL were 15 min and 2.5 m, respectively. The bandwidth of light admitted into the receiver is limited by an interference filter with 1 nm FWHM.

The total linear volume depolarization ratio ( $\delta$ ) at 532 nm is obtained from the ratio of the total backscatter signals (aerosols and molecules). The total backscatter signals are linearly polarized with respect to the plane of polarization of the emitted laser beam. In this paper we define  $\delta$  as

$$\delta = \frac{P_s}{P_p + P_s}, \quad (1)$$

where  $P_p$  and  $P_s$  are the intensities of the parallel- and perpendicular-polarized backscatter signals with respect to the plane of polarization of the outgoing laser beam.

A different definition of the linear volume depolarization ratio ( $\delta_d = P_s/P_p$ ) is used in many other studies (e.g., Freudenthaler et al., 2009).  $\delta_d$ , which is defined separately from the definition we use for  $\delta$  in our work, can be expressed

by the following equation, derived from Eq. (1).

$$\delta_d = \frac{P_s}{P_p} = \frac{\delta}{1 - \delta} \quad (2)$$

This means that the value of  $\delta$  calculated in the study is smaller than  $\delta_d$ .

Although the same signal-detection unit is used to detect both depolarization (backscatter) signals, there may be a difference in the detection efficiency between the channels that detect the parallel- and perpendicular-polarized signals. This difference can be induced by the alignment of the two receiver channels. In order to quantify this effect we carried out a calibration, and we compared  $\delta$  measured by other LIDAR systems under clear sky conditions. The calibration was performed by comparing  $\delta$  measured by other LIDAR systems under clear sky conditions to the values we derived. We set the reference altitude at about 6 km. We obtain a value of 2 % for  $\delta$  by comparing with other lidar measured  $\delta$  result at the reference altitude. This value of 2 % is higher than 0.4 % for molecular scattering,  $\delta_m$  (molecular depolarization ratio) in regions free of aerosols (Weber et al., 1967; Cairo et al., 1999; Behrendt and Nakamura, 2002). This larger measured depolarization of molecular scattering can possibly be interpreted in terms of a channel cross-talk of 1.6 %. However, a characterization of the polarization purity of our lidar system, to be done in the laboratory, is at the moment unavailable to us. The backscatter-depolarization-technique is widely used in atmospheric research with LIDAR because of its capability to distinguish dust from non-dust particles (Noh et al., 2007, 2008, 2012). In the presence of anthropogenic aerosols, the parameter  $\delta$  which is used as a criterion to determine if particles have spherical shape, shows values smaller than 0.05. In contrast, linear depolarization ratios of dust particles range from 0.10 to 0.30 after long-range transport from the dust source regions in central Asia (Sakai et al., 2003; Noh et al., 2007, 2008). The parameter  $\delta$  is the simplest formulation for particle depolarization. However, this parameter is influenced by changes of particle nonsphericity and particle number concentration (Cairo et al., 1999). The aerosol depolarization ratio is calculated as an intensive parameter and it can be used to qualitatively describe the average morphology of the measured aerosol particles.

We apply the equation used by Sakai et al. (2003),

$$\delta_p(z) = \frac{\delta(z)R(z) - \delta_m(z)}{R(z) - 1} \quad (3)$$

The term  $\delta(z)$  is the linear depolarization ratio at altitude  $z$  aboveground. The expression  $\delta_m$  describes the molecular depolarization ratio. We use 0.004. This value takes account of the receiver-channel bandwidth of 1 nm of the system used in our study. The term  $R(z)$  is the height-dependent scattering ratio. This scattering ratio can be written as  $(\beta_a(z) + \beta_m(z))/\beta_m(z)$ . The expression  $\beta_a(z)$  describes the backscatter coefficient of the aerosol particles, and  $\beta_m(z)$  describes

the backscatter coefficient of the atmospheric molecules at altitude  $z$ .

The algorithm of Klett (1981, 1985) was used to retrieve the aerosol extinction and backscatter coefficients, respectively. In this method, the extinction-to-backscatter ratio, the so-called lidar ratio, has to be assumed. To retrieve the appropriate “correct” values of the vertical profiles of the aerosol extinction and backscatter coefficients, we used an iterative inversion approach (by “tuning” the lidar ratio values) based on the inter-comparison of the aerosol optical depth values derived by LIDAR and our AERONET sun/sky radiometer data. We assumed that no stratospheric aerosols were present and that the PBL is homogeneously mixed from ground to 300 m altitude aboveground. This procedure has been used by, e.g. Marenco et al. (1997) and Landulfo et al. (2003). We used the Klett method and we used as input retrieved lidar ratios to retrieve the final values of the aerosol extinction and backscatter coefficients at 532 nm. The difference of the aerosol optical depth derived from our AERONET sun/sky radiometer and our LIDAR data is less than 10 %. The average value (column-mean value) of the lidar ratio obtained from this approach was  $50 \pm 6$  sr for the measurements taken between 4 and 9 May (2009). A similar value for this average lidar ratio was found during the aerosol pollution in spring 2004 and 2005 at the measurement site (Noh et al., 2008). For comparison, highly polluted (light-absorbing) aerosols may show lidar ratios as high as 50–80 sr at 532 nm (Müller et al., 2007; Noh et al., 2011).

Column-integrated aerosol optical depth ( $\tau$ ) at 440 nm and the Ångström exponents (440–870 nm wavelength range, Å) were measured with the polarized-version of the AERONET 318-1 sun/sky radiometer (Holben et al., 1998) at our LIDAR site. Those parameters were retrieved using the AERONET algorithm (Dubovik and King, 2000). Detailed information on the cloud-screening and data-retrieval processes can be found in Dubovik and King (2000) and Smirnov et al. (2000). In this study, we use daily-mean, level 2.0 data which can be downloaded from the AERONET site (<http://aeronet.gsfc.nasa.gov>). The daily number of pollen grains in the atmosphere was monitored by a Burkard 7-day-recording volumetric spore sampler, which was situated on the rooftop of the Gwangju Bohoon Hospital. The building is located 1 km away from the LIDAR site. The sampler is placed at a height of 2 m above the rooftop and at an altitude of 85 m a.m.s.l. Hourly meteorological data such as relative humidity, wind speed, and temperature and PM<sub>10</sub> concentrations were measured at the Gwangju Local Meteorological Administration. The observation height was 250 m a.m.s.l. The administration building is located 5 km away from the LIDAR site. Radiosondes were launched four times a day, at 03:00, 09:00, 15:00, and 21:00 LT by the Korean Meteorological Administration (KMA) at the Gwangju airport which is located about 10 km away from the LIDAR site. The sondes provided us with vertically resolved information on temperature and potential temperature.

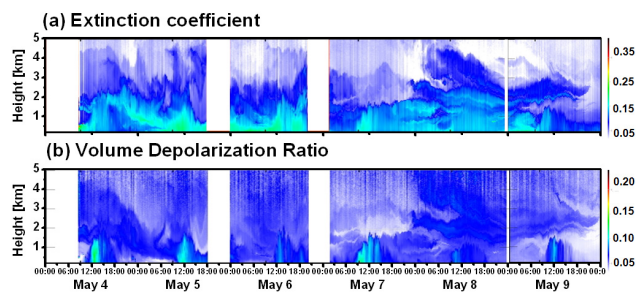


**Fig. 1.** Time-altitude plot of the extinction coefficient (a) and the depolarization ratio (b) at 532 nm, measured from 00:00 LT on 4 May to 24:00 LT on 9 May 2009.

### 3 Relation of pollen concentration to pollen depolarization ratio

Figures 1 and 2 show the temporal variations of the aerosol extinction coefficient ( $\alpha$ ) and the linear volume depolarization ratio ( $\delta$ ) measured by the DPL during the period 4–9 May and 24–29 May 2009. Figure 1a shows high  $\alpha$ -values up to an altitude of 1.5–2.0 km during the complete observation period. The linear volume depolarization ratio  $\delta$  presented in Fig. 1b shows a vertical variation that is different from the variation of  $\alpha$ . The values of  $\delta$  ( $\delta_d$ ) vary between 0.08 (0.09) and 0.13 (0.15) near the surface between 09:00 and 10:00 LT. These- $\delta$  values were measured up to the altitude of 2 km above MSL, which is close to the top of the boundary layer, between 12:00 and 14:00 LT. In contrast, we observed high  $\delta$ -values at lower altitudes, and these  $\delta$ -values were no longer detected after 17:00/18:00 LT. This unique diurnal pattern of the vertical distribution of the  $\delta$ -values was observed over the six consecutive days of our lidar measurements.

Figure 2 shows the background atmospheric conditions. The evolution of the PBL does not show any significant increase of  $\delta$  during noon. A similar vertical distribution and similar values of  $\alpha$  were observed, see Fig. 2a. However, low values (less than 0.05) of  $\delta$  were observed throughout these 6 days of lidar measurements, and there was no specific diurnal pattern visible, see Fig. 2b.

The aerosol depolarization ratio ( $\delta_p$ ) was calculated in terms of hourly-mean values for the time from 09:00 to 17:00 LT during the period the diurnal pattern was observed. Figure 3 shows hourly calculated values of  $\delta_p$ ,  $\delta$ , and the aerosol backscatter coefficient at 532 nm. The largest differences between  $\delta_p$  and  $\delta$  were observed between 12:00 and 14:00 LT.

The large value of  $\delta$  indicates the dominance of non-spherical aerosols at the measurement site. In general, a large value of  $\delta$  can be induced by Asian dust and sea salt, too. In the case of Asian dust events, the value of  $\delta$  is higher than 0.15 in most cases (Noh et al., 2008; Sakai et al., 2003), and

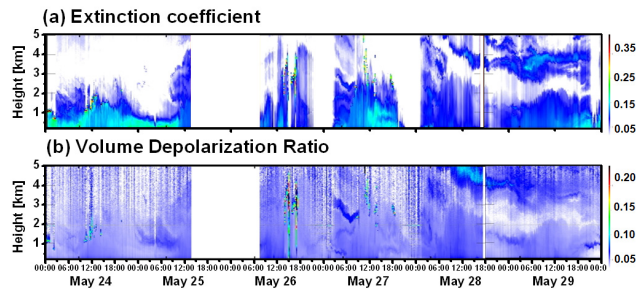


**Fig. 2.** Time-altitude plot of the extinction coefficient (a) and the depolarization ratio (b) at 532 nm measured from 00:00 LT on 24 May to 24:00 LT on 29 May 2009.

the vertical distribution of  $\delta$  in general is well correlated with  $\alpha$ . In addition, Asian dust is usually found above the planetary boundary layer. The production mechanism of airborne Asian dust cause large amounts of dust particles transported out of the PBL into the free troposphere where it is undergoing long-range transport in comparably high altitudes (Noh et al., 2008; Shimizu et al., 2004). In general, we do not observe Asian dust only within the planetary boundary layer. Asian dust is often observed to reach the altitude higher than 2 km since Asian dust is long-range transported from China in this measurement site (Noh et al., 2012; Sakai et al., 2003).

We used surface  $PM_{10}$  data and sun/sky radiometer data to identify non-spherical particle types that we assumed to increase  $\delta_p$  during the measurement period. Figure 4 shows hourly variations of the surface  $PM_{10}$  concentration. Figure 4 also shows aerosol optical depth ( $\tau$ ) at 440 nm and the Ångström exponent ( $\text{Å}$ ) in the wavelength-range from 440 to 870 nm measured by our sun/sky radiometer for the period 4–9 May. The average values of  $\delta_p$  between 0.3 to 1 km altitude aboveground are also shown in Fig. 4.  $PM_{10}$  concentrations rapidly increased to values as large as  $100 \mu\text{g m}^{-3}$  by 10 May. Values of  $\tau$  and  $\text{Å}$  ranged from 0.28 to 0.91 and from 1.12 to 1.44, respectively. In northeast Asia, during the Asian dust period,  $PM_{10}$  concentrations and values of  $\tau$  tend to increase, whereas  $\text{Å}$  shows values smaller than 1 (Murayama et al., 2001).

Figure 5a and b show the relationship between  $\delta_p$  and aerosol optical depth respectively the  $PM_{10}$  concentration. The aerosol optical depth was calculated by integrating the aerosol extinction coefficient from 0.3 to 1.0 km, which is the same altitude range for which we have data on  $\delta_p$ . The correlation coefficients between  $\delta_p$  and aerosol optical depth and between  $\delta_p$  and  $PM_{10}$  are 0.0047 and  $-0.01$ , respectively. For this comparison we used all data collected during the 6 days of observation. Figure 5a shows that the increase of  $\delta_p$  was not induced by the increase of aerosol concentration. Figure 5b also indicated that the  $PM_{10}$  concentration does not seem to be related with  $\delta_p$ . We think that this increase of  $\delta$  is not caused by Asian dust, because we find high  $\text{Å}$ -values, ranging from 1.20 to 1.43 during 4–9 May. The

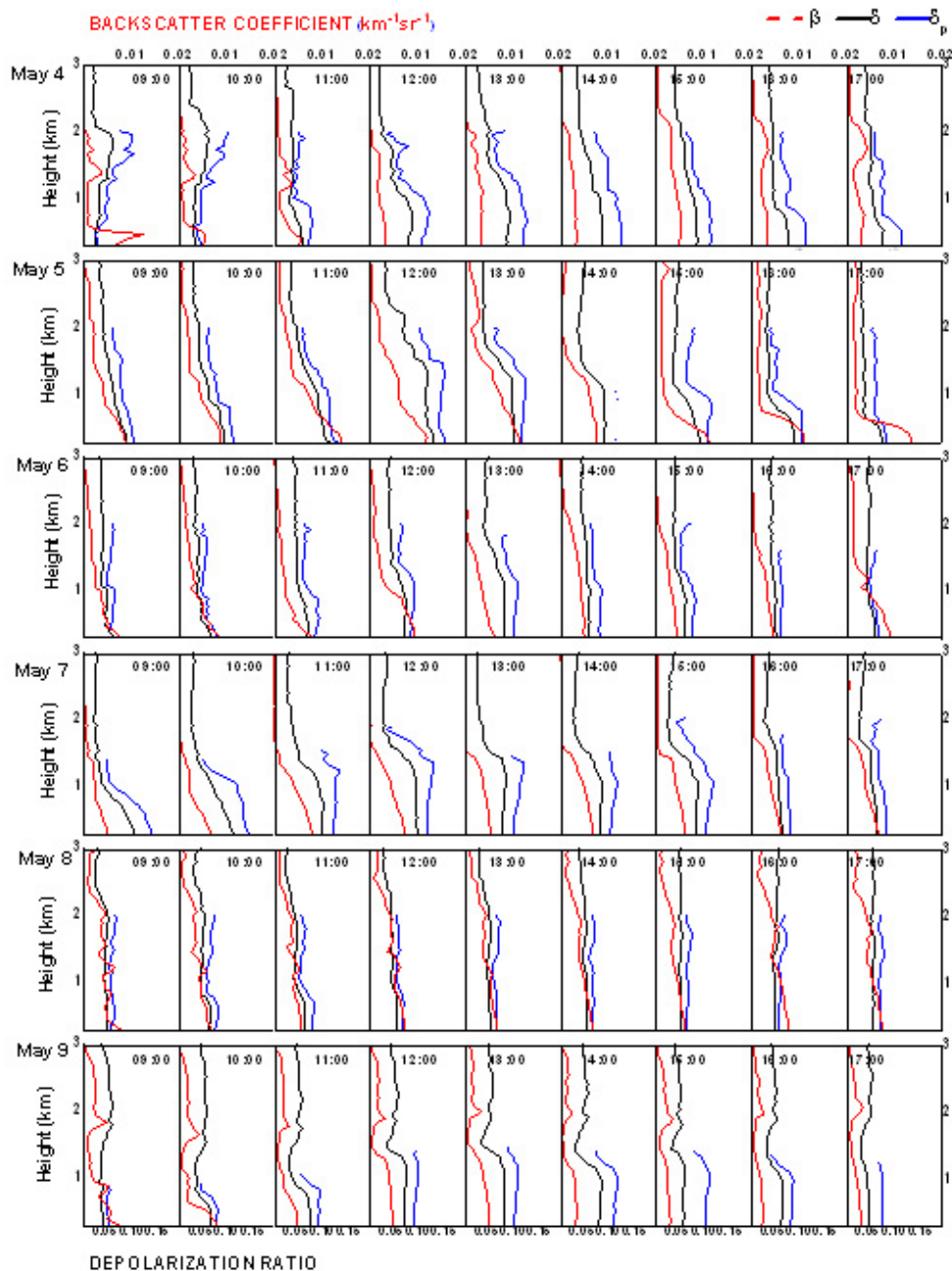


**Fig. 3.** Diurnal variation of hourly averaged aerosol backscattering coefficients, depolarization ratios, and linear particle depolarization ratios measured from 09:00 to 17:00 LT.

Å-data, and the difference between the diurnal pattern of the vertical distribution of  $\delta$  and  $\alpha$  indicate that the diurnal and vertical characteristics of  $\delta$  (Fig. 1b) can hardly be attributed to Asian dust.

Locally wind-blown dust may also cause elevated values of  $\delta_p$ . However, we do not think that this was a major source for the increased values of  $\delta_p$  since our measurement site is surrounded by mountains and buildings. In particular, Fig. 2b shows that  $\delta$  was not increased even with the comparably

windy condition that were present around noon. The different  $\delta$ -values that prevailed during the same windy conditions imply that  $\delta$  was not influenced by wind-blown dust during the measurement period. In particular, if wind-blown dust had affected our measurement site,  $\delta_p$  would have shown a correlation with  $PM_{10}$ . However, no correlation was found between  $PM_{10}$  and  $\delta_p$ , see Fig. 5.

Another cause of elevated values of  $\delta_p$  could be sea salt. Sea salt shows values of  $\delta_p$  of 0.08 to 0.1 (Sakai et al., 2010;

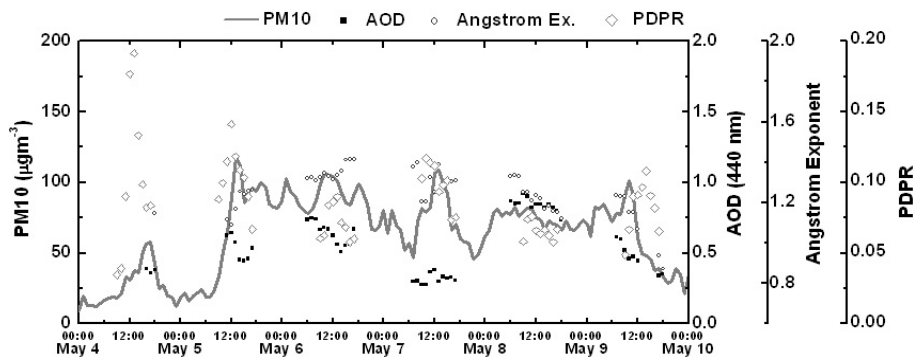


**Fig. 4.** Hourly averaged  $\text{PM}_{10}$  concentration (solid line) measured from 4–10 May 2009. Also shown are aerosol optical depth at 440 nm (dark square) and the Ångström exponent (open circle, wavelength range 440–870 nm) measured by the AERONET sun/sky radiometer. PDPR (open diamond) denotes the linear particle depolarization ratio.

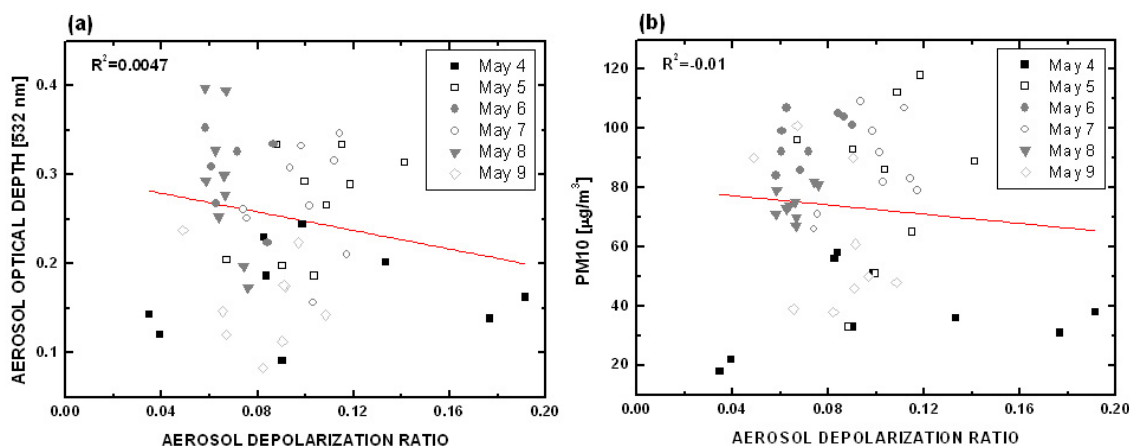


**Fig. 5.** Correlation between (a) the pollen depolarization ratio and aerosol optical depth and (b) between linear aerosol depolarization ratio and  $\text{PM}_{10}$  concentration.

Murayama et al., 1999), which is lower than what we observed. In addition, it is rather unlikely that significant concentrations of sea-salt particles were transported to the observation site, in view of the location of the measurement site, which is 50 km away from the coastline and shielded by mountains. In addition, if we consider the repeating diurnal and vertical pattern of the observed values of  $\delta$ , it is also less likely that sea salt had a dominant influence on  $\delta$ . Previous studies (Lee et al., 2008; Park et al., 2007) do not report on a significant contribution of sea salt to the  $\text{PM}_{10}$  concentrations at our measurement site, which also corroborates or assumption that the contribution of sea salt was insignificant.

For all the reasons mentioned above we therefore attempted to identify a relationship between increased values  $\delta$  and the presence of pollen. Such a relationship was already discussed in a study by Sassen (2008). The physical shape of pollen particles is known to be nearly spherical or non-spherical (Hong, 1983; Treloar et al., 2004). The diameter ranges from 16 to 50  $\mu\text{m}$  according to Bhat and Rajasab (1989). The smallest pollen grains, forget-me-not

(*Myosotis* spp.), is around 6  $\mu\text{m}$  in diameter. However, this kind of pollen was not observed during our study period. Figure 6 shows a microscope image of pollens detected with high concentration around our measurement site in spring. The pollen from pine trees was most dominant at the measurement site during the observation period, while pollen of oak trees was the second-most abundant type of pollen. *Betula* and *Ulmus* were also found to contribute to high pollen counts during the observation period. Thus we believe that pollen for the main part originated from the forest near our measurement site. As shown in Fig. 6, pollen from pine pine and oak trees, which were found to contribute most to the high pollen number concentrations, have non-spherical shape. The pollen size ranges from 45–70 and 28–38  $\mu\text{m}$  in diameter, respectively.

Figure 7 shows daily pollen concentrations for the times from 4–9 and 24–31 May 2009. During the six-day observation period, we found high surface pollen concentrations between 1216 and 1952  $\text{m}^{-3}$  from 4 to 7 May. Values of 346 and 220  $\text{m}^{-3}$  were measured on 8 and 9 May, respectively.

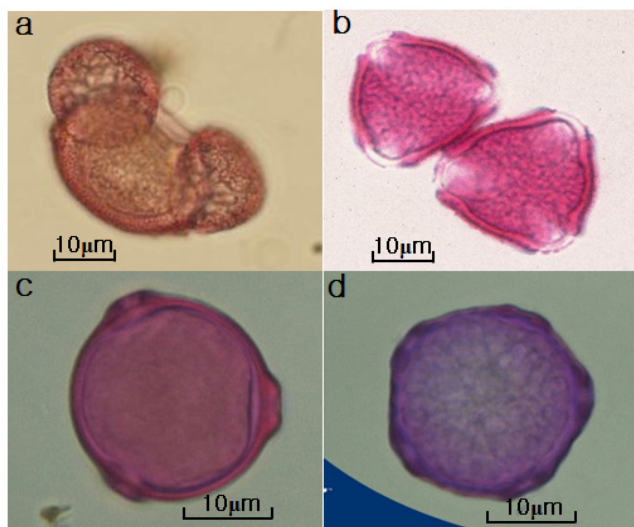


**Fig. 6.** Microphotographs of pollen grain observed in this study: (a) pine, (b) quercus, (c) betula, (d) ulmus.

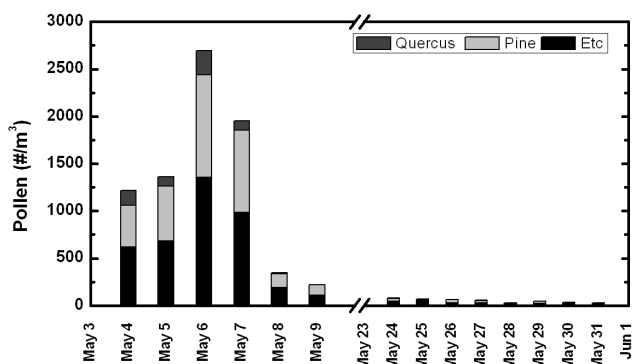


**Fig. 7.** Daily distribution of pollen counts from 4 to 9 May and from 24 to 31 May at Gwangju, Korea.

These latter two numbers are still larger than the ones we found during observations carried out from 10 to 31 May. Figure 4 shows that  $\delta$  did not increase during the period from 24–31 May when the pollen concentration was observed to be lower than  $100 \text{ m}^{-3}$ . The enhanced  $\delta$ -values (see Fig. 1b) could thus be attributed to the increased pollen concentration that was observed during the period 4–9 May. However, the increased pollen concentration did not affect the  $\text{PM}_{10}$  variation because the  $\text{PM}_{10}$  sampler has a cut-off diameter for aerosols with aerodynamic diameter larger than  $10 \mu\text{m}$ . This value is significantly smaller than the diameter of the pollen that dominated during our observation period. Given the high  $\text{PM}_{10}$  concentration that reached  $100 \mu\text{g m}^{-3}$  the enhanced aerosol extinction coefficient could be affected by haze transported from the Chinese mainland, see for example to the measurement site in Gwangju (Noh et al., 2009, 2011).

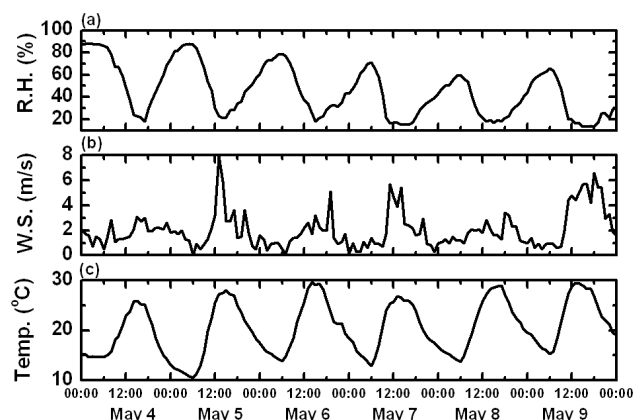


**Fig. 8.** Hourly averaged meteorological data taken from 00:00 on 4 May to 24:00 on 9 May 2009. (a) Relative humidity, (b) wind speed, and (c) temperature.

#### 4 Effects of the meteorological conditions on the diurnal and vertical patterns of pollen

Alba et al. (2000), Jato et al. (2000), Käpylä (1984) and Bartková-Ščevková (2003) report that the air temperature, the duration (hours) of sunshine, and the wind speed positively affect the atmospheric concentration of pollen during the main pollen season. In contrast, rainfall and humidity tend to decrease pollen concentrations during pollination periods. Käpylä (1984) and Latorre and Caccavari (2009) report that maximum pollen concentrations are observed around noon if air temperature reaches its maximum and relative humidity is at minimum. These previous studies for the most part took place near forests or in mountain areas of the Northern Hemisphere.

The diurnal variation of the meteorological conditions, see Fig. 8, are similar to the ones that prevailed during the investigations carried out by Käpylä (1984) and Latorre and Caccavari (2009). These conditions allow us to interpret the hourly variations of the pollen concentration. Relative humidity decreased from 60–80 % to less than 20 % between 09:00 and 12:00 LT. Air temperature increased from  $15^\circ\text{C}$  at 09:00 LT to above  $25^\circ\text{C}$  at around 13:00 LT. Between 16:00 and 09:00 LT next day relative humidity increased, and its maximum value was observed at dawn whereas temperature decreased during that time. Mean wind speeds were  $3.1$  and  $2.8 \text{ m s}^{-1}$  on 4 and 8 May, respectively, which are lower than those on the other days. Still we observed an increase of temperature during the daytime on these two days. Variations of  $\delta$  at 0.3 km, which is the lowest observable altitude, show a strong correlation with increasing temperature and decreasing relative humidity, see Figs. 1b and 3.

The increase of  $\delta$  is thought to be caused by the increase of the pollen load in the atmosphere. The maximum pollen concentration was observed around noontime when the highest air temperature and the lowest relative humidity was reached.

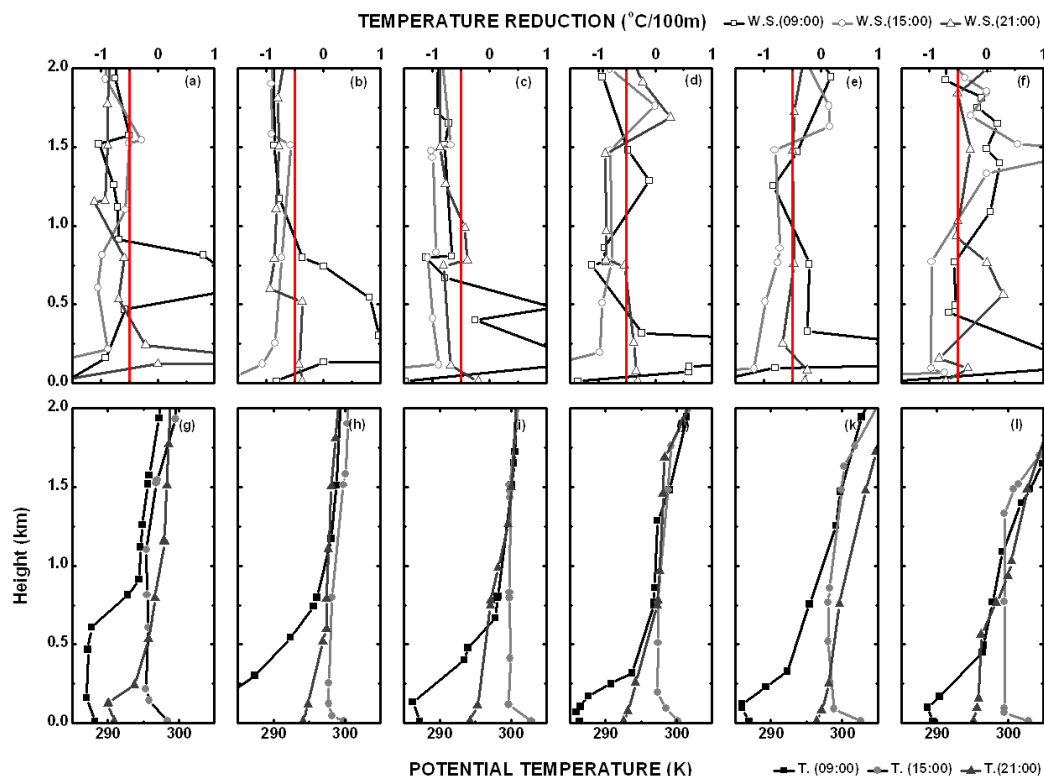


**Fig. 9.** Radiosonde data taken on 4 May (a, g), 5 May (b, h), 6 May (c, i), 7 May (d, j), 8 May (e, k), and 9 May (f, l). Temperature decrease observed on 09:00 (open square), 15:00 LT (open circle) and 21:00 LT (open triangle). Potential temperature observed on 09:00 LT (closed square), 15:00 LT (closed circle) and 21:00 LT (closed triangle).

There are still uncertainties in identifying the reasons for the observed diurnal patterns of the pollen at the surface, if we look at the meteorological data. The same diurnal pattern of meteorological conditions was observed during the measurement period as shown in Fig. 2. The depolarization ratio, however, was not large during this period as shown in Fig. 2b. The number concentration of pollen was also low, see Fig. 7. We assume that most of the pollen had been released into the atmosphere during the a pollination period that preceded our observation time.

The altitude range up to which pollen was observed varied significantly between 09:00 and 18:00 LT, see Figs. 1b and 3. Pollen started to be observed near the surface around 09:00 LT, reached heights up to 2 km around 13:00 LT, and was mainly present near the surface around 18:00 LT during 6 consecutive days. This kind of diurnal pattern of the vertical distribution of pollen is thought to be related to short- and long-distance travel characteristics. Most of the pollen grains injected into the air will fall to the ground near their source. Only a few pollen, termed the “escape fraction” (Gregory, 1978), will be carried over long distances. Gregory (1978) reports that only 10 % of the total pollen number released into the air can be dispersed across long distances. For this to happen, vertical transport is needed. According to Mandrioli

et al. (1984), this vertical movement of atmospheric particles requires atmospheric turbulence. Turbulence results from the vertical movement of air masses within the planetary boundary layer when the surface is heated after sunrise. Thus, the increase of  $\delta$  with altitude seems to be associated with vertical mixing via turbulent transport.

Vertically resolved temperature reduction (the decreasing rate of temperature per 100 m altitude) and potential temperature measured with radiosonde, see Fig. 9, corroborate our assumption that the diurnal pattern of the vertical distribution of pollen was caused by turbulent transport. Lower temperature reduction than  $-0.5$  was observed only near the surface at 09:00 and 21:00 LT. It means that turbulent mixing did not take place at that time. On the contrary, turbulent mixing was thought to be active as the low value of temperature reduction was observed over the altitude interval between the surface and 1.0 or 1.5 km at 15:00 LT.

The rate of increase of potential temperature at 15:00 LT also supports our assumption that turbulent mixing occurred during that time. Radiosonde data were taken at 6 h intervals only. This measurement cycle still allows us to conclude that the altitude range in which the atmosphere as unstable induced vertical mixing of atmospheric aerosols.

## 5 Conclusions

In this study we used the linear volume depolarization ratio measured with LIDAR and meteorological data to explain the diurnal pattern of the vertical distribution of biogenic pollen. Based on LIDAR measurements, the linear particle depolarization ratio of pollen was between 0.08 to 0.20 at 532 nm wavelength. These numbers are significantly larger than those of anthropogenic aerosols. The linear particle depolarization ratio, which was around 0.06 in the morning hours started to increase around 09:00 LT. The maximum values were measured between 12:00 and 14:00 LT when air temperature reached its maximum. The linear particle depolarization ratio decreased again after 14:00 LT. In terms of the vertical distribution, high values of the linear particle depolarization ratio were observed in the lowest 500 m aboveground at 9:00 LT. High values were found to altitudes of 1.5–2.0 km aboveground around noontime. The altitude, where high particle depolarization ratios were detected, decreased in the afternoon. After 18:00 LT linear particle depolarization ratios again reached their minimum values. Moreover, large linear particle depolarization ratios were only found within the planetary boundary layer, i.e., up to 2 km aboveground, which implies that long-range transport of pollen can hardly reach the free troposphere through dispersion processes.

The diurnal variability and the vertical distribution of pollen observed in this study can be utilized as a reference to separate pollen from mineral dust particles, which could be necessary for space-borne sensors such CALIPSO (Cloud-Aerosol Lidar and Infrared Pathfinder Satellite Observations) in areas where significant pollen production and long-range transport of dust occur. Moreover, continuous measurements of the diurnal and vertical characteristics of pollen can be used to improve the accuracy of pollen forecasting model by using these data in data assimilation studies.

*Acknowledgements.* This work was funded by the Korea Meteorological Administration Research and Development Program under Grant CATER 2012-7080. This work was supported by the project “Reconstruction and observation of components for the Southern and Northern Annular Mode to investigate the cause of polar climate change (PE13010)” of the Korea Polar Research Institute. Sungkyun Shin is supported by the Global Ph.D. Fellowship program, which is sponsored by the National Research Foundation of Korea.

Edited by: F. Fierli

## References

- Adams-Groom, B., Emberlin, J., Corden, J., Millington, W., and Mullins, J.: Predicting the start of the birch pollen season at London, Derby and Cardiff, United Kingdom, using a multiple regression model, based on data from 1987 to 1997, *Aerobiologia*, 18, 117–123, 2002.
- Alba, F., De La Guardia, C. D., and Comtois, P.: The effect of meteorological parameters on diurnal patterns of airborne olive pollen concentration, *Grana*, 39, 200–208, 2000.
- Andersen, T. B.: A model to predict the beginning of the pollen season, *Grana*, 30, 269–275, 1991.
- Bartková-Ščevková, J.: The influence of temperature, relative humidity and rainfall on the occurrence of pollen allergens (*Betula*, Poaceae, *Ambrosia artemisiifolia*) in the atmosphere of Bratislava (Slovakia), *Int. J. Biometeorol.*, 48, 1–5, 2003.
- Beggs, P.: Impacts of climate change on aeroallergens: past and future, *Clinical & Experimental Allergy*, 34, 1507–1513, 2004.
- Behrendt, A. and Nakamura, T.: Calculation of the calibration constant of polarization lidar and its dependency on atmospheric temperature, *Optics Express*, 10, 805–817, 2002.
- Bhat, M. M. and Rajasab, A. H.: Efficiency of Vertical Cylinder Spore Trap and Seven Day Volumetric Burkard Spore Trap in Monitoring Airborne Pollen and Fungal Spores, *Grana*, 28, 147–153, 1989.
- Cairo, F., Di Donfrancesco, G., Adriani, A., Pulvirenti, L., and Fierli, F.: Comparison of various linear depolarization parameters measured by lidar, *Applied Optics*, 38, 4425–4432, 1999.
- D’Amato, G. and Cecchi, L.: Effects of climate change on environmental factors in respiratory allergic diseases, *Clinical Experiment. Allergy*, 38, 1264–1274, 2008.
- Damialis, A., Gioulekas, D., Lazopoulou, C., Balafoutis, C., and Vokou, D.: Transport of airborne pollen into the city of Thessaloniki: the effects of wind direction, speed and persistence, *Int. J. Biometeorol.*, 49, 139–145, 2005.
- Dubovik, O. and King, M. D.: A flexible inversion algorithm for retrieval of aerosol optical properties from Sun and sky radiance measurements, *J. Geophys. Res.*, 105, 673–620, 2000.
- Esch, R. and Bush, R.: *Aerobiology of outdoor allergens*, edited by: Adkinson Jr., N. F., Yunginger, J. W., Busse, W. W., Bochner, B. S., Holgate, S. T., Simons, F. E., Middleton’s allergy principles and practice, 6th Edn., St. Louis, Mosby, 529–555, 2003.
- Frøsig, A. and Rasmussen, A.: *Astma-Allergi Forbundet Pollen- & Sporemålinger i Danmark Sæsonen 2001*, Danish Meteorological Institute Technical report, 35, 2003.
- Freudenthaler, V., Esselborn, M., Wiegner, M., Heese, B., Tesche, M., Ansmann, A., Müller, D., Althausen, D., Wirth, M., Fix, A., Ehret, G., Knippertz, P., Toledano, C., Gasteiger, J., Garhammer, M., and Seefeldner, M.: Depolarizationratio profiling at several wavelengths in pure Saharan dust during SAMUM 2006, *Tellus B*, 61, 165–179, doi:10.1111/j.1600-0889.2008.00396.x, 2009.
- Giner, M. M., Carrión García, J. S., and García Sellés, J.: Aerobiology of *Artemisia* airborne pollen in Murcia (SE Spain) and its relationship with weather variables: annual and intradiurnal variations for three different species. Wind vectors as a tool in determining pollen origin, *Int. J. Biometeorol.*, 43, 51–63, 1999.
- Gioulekas, D., Damialis, A., Papakosta, D., Syrigou, A., Mpaka, G., Saxoni, F., and Patakas, D.: 15-Year aeroallergen records. Their usefulness in Athens Olympics, 2004, *Allergy*, 58, 933–938, 2003.

- Gregory, P.: Distribution of airborne pollen and spores and their long distance transport, *Pure Appl. Geophys.*, 116, 309–315, 1978.
- Hart, M., Wentworth, J., and Bailey, J.: The effects of trap height and weather variables on recorded pollen concentration at Leicester, *Grana*, 33, 100–103, 1994.
- Hjelmroos, M.: Evidence of long-distance transport of *Betula* pollen, *Grana*, 30, 215–228, 1991.
- Holben, B., Eck, T., Slutsker, I., Tanre, D., Buis, J., Setzer, A., Vermote, E., Reagan, J. A., Kaufman, Y. J., Nakajima, T., Lavenu, F., Jankowiak, I., and Smirnov, A.: AERONET-A federated instrument network and data archive for aerosol characterization, *Remote Sens. Environ.*, 66, 1–16, 1998.
- Hong, D.: On pollen shape in some groups of dicotyledons, *Grana*, 22, 73–78, 1983.
- Jato, M., Rodríguez, F., and Seijo, M.: *Pinus* pollen in the atmosphere of Vigo and its relationship to meteorological factors, *Int. J. Biometeorol.*, 43, 147–153, 2000.
- Käpylä, M.: Diurnal variation of tree pollen in the air in Finland, *Grana*, 23, 167–176, 1984.
- Kasprzyk, I.: Comparative study of seasonal and intradiurnal variation of airborne herbaceous pollen in urban and rural areas, *Aerobiologia*, 22, 185–195, 2006.
- Klett, J. D.: Stable analytical inversion solution for processing lidar returns, *Applied Optics*, 20, 211–220, 1981.
- Klett, J. D.: Lidar inversion with variable backscatter/extinction ratios, *Applied Optics*, 24, 1638–1643, 1985.
- Kim, K. W.: Physico-chemical characteristics of visibility impairment by airborne pollen in an urban area, *Atmos. Environ.*, 41, 3565–3576, 2007.
- Laaidi, K.: Predicting days of high allergenic risk during *Betula* pollination using weather types, *Int. J. Biometeorol.*, 45, 124–132, 2001.
- Laaidi, M., Thibaudon, M., and Besancenot, J. P.: Two statistical approaches to forecasting the start and duration of the pollen season of *Ambrosia* in the area of Lyon (France), *Int. J. Biometeorol.*, 48, 65–73, 2003.
- Landulfo, E., Papayannis, A., Artaxo, P., Castanho, A. D. A., de Freitas, A. Z., Souza, R. F., Vieira Junior, N. D., Jorge, M. P. M. P., Sánchez-Ccoyllo, O. R., and Moreira, D. S.: Synergetic measurements of aerosols over São Paulo, Brazil using LIDAR, sunphotometer and satellite data during the dry season, *Atmos. Chem. Phys.*, 3, 1523–1539, doi:10.5194/acp-3-1523-2003, 2003.
- Latorre, F. and Caccavari, M. A.: Airborne pollen patterns in Mar del Plata atmosphere (Argentina) and its relationship with meteorological conditions, *Aerobiologia*, 25, 297–312, 2009.
- Lee, H., Park, S. S., Kim, K. W., and Kim, Y. J.: Source identification of PM<sub>2.5</sub> particles measured in Gwangju, Korea, *Atmos. Res.*, 88, 199–211, 2008.
- Lewis, W. H., Vinay, P., and Zenger, V. E.: Airborne and allergenic pollen of North America, The Johns Hopkins University Press Baltimore & London, 105–127, 1983.
- Mandrioli, P., Negrini, M. G., Cesari, G., and Morgan, G.: Evidence for long range transport of biological and anthropogenic aerosol particles in the atmosphere, *Grana*, 23, 43–53, 1984.
- Marengo, F., Santacesaria, V., Bais, A., Balis, D., di Sarra, D., Papayannis, A., and Zerefos, C. S.: Optical properties of tropospheric aerosols determined by lidar and spectrophotometric measurements (PAUR campaign), *Applied Optics*, 36, 6785–6886, 1997.
- Müller, D., Ansmann, A., Mattis, I., Tesche, M., Wandinger, U., Althausen, D., and Pisani, G.: Aerosol-type-dependent lidar ratios observed with Raman lidar, *J. Geophys. Res.*, 112, D16202, doi:10.1029/2010JD014873, 2007.
- Murayama, T., Okamoto, H., Kaneyasu, N., Kamataki, H., and Miura, K.: Application of lidar depolarization measurement in the atmospheric boundary layer: Effects of dust and sea-salt particles, *J. Geophys. Res.*, 104, 31781–31792, doi:10.1029/1999JD900503, 1999.
- Murayama, T., Sugimoto, N., Uno, I., Kinoshita, K., Aoki, K., Hagiwara, N., Liu, Z., Matsui, I., Sakai, T., Shibata, T., Arai, K., Shon, B.-J., Won, J.-G., Yoon, S.-C., Li, T., Zhou, J., Hu, H., Abo, M., Iokibe, K., Koga, R., and Iwasaka, Y.: Ground-based network observation of Asian dust events of April 1998 in east Asia, *J. Geophys. Res.*, 106, 18345–18360, 2001.
- Noh, Y. M., Kim, Y. J., Choi, B. C., and Murayama, T.: Aerosol lidar ratio characteristics measured by a multi-wavelength Raman lidar system at Anmyeon Island, Korea, *Atmos. Res.*, 86, 76–87, 2007.
- Noh, Y. M., Kim, Y. J., and Müller, D.: Seasonal characteristics of lidar ratios measured with a Raman lidar at Gwangju, Korea in spring and autumn, *Atmos. Environ.*, 42, 2208–2224, 2008.
- Noh, Y. M., Müller, D., Mattis, I., Lee, H., and Kim, Y. J.: Vertically resolved light-absorption characteristics and the influence of relative humidity on particle properties: Multiwavelength Raman lidar observations of East Asian aerosol types over Korea, *J. Geophys. Res.*, 116, D06206, doi:10.1029/2010JD014873, 2011.
- Noh, Y. M., Müller, D., Lee, H., Lee, K. H., Kim, K., Shin, S., and Kim, Y. J.: Estimation of radiative forcing by the dust and non-dust content in mixed east asian pollution plumes on the basis of depolarization ratios measured with lidar, *Atmos. Environ.*, 61, 221–231, 2012.
- Park, K., Kim, H., Kim, K., Oh, J., Lee, S., and Choi, Y.: Characteristics of regional distribution of pollen concentration in Korean Peninsula, *Korean J. Agr. Forest Meteorol.*, 10, 167–176, 2008.
- Park, S. S., Kim, Y. J., and Kang, C. H.: Polycyclic aromatic hydrocarbons in bulk PM<sub>2.5</sub> and size-segregated aerosol particle samples measured in an urban environment, *Environ. Monitor. Assess.*, 128, 231–240, 2007.
- Porsbjerg, C., Rasmussen, A., and Backer, V.: Airborne pollen in Nuuk, Greenland, and the importance of meteorological parameters, *Aerobiologia*, 19, 29–37, 2003.
- Rantio-Lehtimäki, A. and Matikainen, E.: Pollen allergen reports help to understand pre-season symptoms, *Aerobiologia*, 18, 135–140, 2002.
- Raynor, G. S., Ogden, E. C., and Hayes, J. V.: Variation in ragweed pollen concentration to a height of 108 meters, *J. Allergy Clinical Immunol.*, 51, 199–207, 1973.
- Raynor, G. S., Hayes, J. V., and Ogden, E. C.: Particulate dispersion into and within a forest, *Bound.-Lay. Meteorol.*, 7, 429–456, 1974.
- Raynor, G. S., Hayes, J. V., and Ogden, E. C.: Particulate dispersion from sources within a forest, *Bound.-Lay. Meteorol.*, 9, 257–277, 1975.
- Sakai, T., Nagai, T., Nakazato, M., Mano, Y., and Matsumura, T.: Ice clouds and Asian dust studied with lidar measurements of particle extinction-to-backscatter ratio, particle depolarization, and water-vapor mixing ratio over Tsukuba, *Applied Optics*, 42,

- 7103–7116, 2003.
- Sakai, T., Nagai, T., Zaizen, Y., and Mano, Y.: Backscattering linear depolarization ratio measurements of mineral, sea-salt, and ammonium sulfate particles simulated in a laboratory chamber, *Applied Optics*, 49, 4441–4449, 2010.
- Sassen, K.: Boreal tree pollen sensed by polarization lidar: depolarizing biogenic chaff, *Geophys. Res. Lett.*, 35, L18810, doi:10.1029/2008GL035085, 2008.
- Severova, E. and Polevova, S.: Aeropalynological calendar for Moscow 1994, *Ann. Agr. Environ. Medicine*, 3, 115–120, 1996.
- Shea, K. M., Truckner, R. T., Weber, R. W., and Peden, D. B.: Climate change and allergic disease, *J. Allergy Clinical Immun.*, 122, 443–453, 2008.
- Shimizu, A., Sugimoto, N., Matsui, I., Arao, K., Uno, I., Murayama, T., Kagawa, N., Aoki, K., Uchiyama, A., and Yamazaki, A.: Continuous observations of Asian dust and other aerosols by polarization lidars in China and Japan during ACE-Asia, *J. Geophys. Res. Atmos.* (1984–2012), 109, D19S17, doi:10.1029/2002JD003253, 2004.
- Smirnov, A., Holben, B., Eck, T., Dubovik, O., and Slutsker, I.: Cloud-screening and quality control algorithms for the AERONET database, *Remote Sens. Environ.*, 73, 337–349, 2000.
- Sofiev, M., Siljamo, P., Ranta, H., and Rantio-Lehtimäki, A.: Towards numerical forecasting of long-range air transport of birch pollen: theoretical considerations and a feasibility study, *Int. J. Biometeorol.*, 50, 392–402, 2006.
- Treloar, W. J., Taylor, G. E., and Flenley, J. R.: Towards automation of palynology I: analysis of pollen shape and ornamentation using simple geometric measures, derived from scanning electron microscope images, *J. Quaternary Sci.*, 19, 745–754, 2004.
- Vázquez, L., Galán, C., and Domínguez-Vilches, E.: Influence of meteorological parameters on olea pollen concentrations in Córdoba (South-western Spain), *Int. J. Biometeorol.*, 48, 83–90, 2003.
- Water, P. K. V., Keever, T., Main, C. E., and Levetin, E.: An assessment of predictive forecasting of *Juniperus ashei* pollen movement in the Southern Great Plains, USA, *Int. J. Biometeorol.*, 48, 74–82, 2003.
- Weber, A., Porto, S. P. S., Cheesman, L. E., and Barrett, J. J.: High-resolution Raman spectroscopy of gases with cw-laser excitation, *J. Optic. Soc. Am.*, 57, 19–27, 1967.
- WHO: World Health Report 2003: A Vision for Global Health, Shaping the Future, World Health Organization, 2003.